Available online at www.sciencedirect.com
ScienceDirect
Applied Surface Science 254 (2008) 3626–3629
applied surface science
www.elsevier.com/locate/apsusc

Electrical and ellipsometry study of sputtered SiO_2 structures with embedded Ge nanocrystals

P. Basa [a], A.S. Alagoz [b], T. Lohner [a], M. Kulakci [b], R. Turan [b], K. Nagy [a], Zs.J. Horváth [a,*]

[a] *Hungarian Academy of Sciences, Research Institute for Technical Physics and Materials Science, P.O. Box 49, H-1525 Budapest, Hungary*
[b] *Middle East Technical University, Inonu Blvrd., TR-06531 Ankara, Turkey*

Available online 1 November 2007

Abstract

SiO_2 layer structures with a middle layer containing Ge nanocrystals were prepared by sputtering on n- and p-type Si substrates, and by consecutive annealing. Ge content in the middle layer was varied in the range of 40–100%. Most of the structures exhibited low breakdown voltages. The current through the structures became Schottky-like after breakdown. However, some p-type samples showed a considerable memory effect. It was obtained by spectroscopic ellipsometry that the middle layer contains amorphous Ge phase as well. The results also suggest intermixing of the layers during the sputtering and/or the annealing process.

PACS : 81.15.Cd; 81.05−t; 78.67.Bf; 78.20.−e

Keywords: Sputtering; SiO_2 structure; Annealing; Ge nanocrystals

1. Introduction

Ge nanocrystals embedded in dielectrics are widely studied for memory and LED purposes [1–11]. As non-volatile memory devices are concerned, one of the ways used for replacing the floating gate is the application of semiconductor nanocrystals embedded in dielectrics as the charge storage medium. Ge nanocrystals are good candidates for this purpose [1–3]. Successful photoluminescence experiments show that these structures are promising solutions for light emitting applications as well [4–6]. One of the methods used for creating Ge nanocrystals is the electron beam evaporation of a thin Ge layer and the subsequent rapid thermal annealing of the structure [1,3]. Another processes involve chemical etching [4], Ge ion implantation [7], sputtering [2,5,6,8], molecular beam epitaxy combined with rapid thermal processing [9], or plasma enhanced chemical vapour deposition [10].

In this work SiO_2 layer structures with Ge nanocrystals have been prepared by sputtering on n- and p-type Si substrates with a thin surface oxide layer of 4 nm. Ge content has been varied to study its effect on the electrical and optical properties.

2. Experimental

First a 4 nm thermal oxide was grown. It was covered with a 20 nm thick SiO_2 layer containing Ge and with a 40 nm thick SiO_2 layer without any Ge content by sputtering. The effect of Ge content was studied in the range of 40–100% (see Tables 1 and 2). The schematic of studied structures is presented in Fig. 1. All the structures were annealed at 750 °C for 30 min. For electrical measurements, capacitors were formed with an area of 0.8 mm × 0.8 mm by evaporation of Al onto the front side of the wafer. Backside ohmic contacts were also prepared by evaporation of Al after appropriate chemical treatments [12,13].

The thickness and nanocrystal content of the layers were studied by spectroscopic ellipsometry, while their electrical behaviour by current–voltage (*I–V*), capacitance–voltage (*C–V*), and conductance–voltage (*G–V*) measurements at room temperature in dark. *C–V* and *G–V* measurements were performed at a frequency of 1 MHz.

3. Results and discussion

Most of the studied structures exhibited low breakdown voltage in the range of 3–5 V independent of the Ge content.

* Corresponding author. Tel.: +36 1 3922683; fax: +36 1 3922235.
E-mail address: horvzsj@mfa.kfki.hu (Zs.J. Horváth).

0169-4332/$ – see front matter © 2007 Published by Elsevier B.V.
doi:10.1016/j.apsusc.2007.10.075

Table 1
Nominal Ge concentration, type and orientation of the substrates, layer thicknesses and composition obtained by spectroscopic ellipsometry and mean square error (MSE) of the fit using model "1"

Sample name	Nominal Ge concentration (%)	Type/orientation	Top SiO_2 thickness (nm)	(c-Ge + SiO_2) thickness (nm)	c-Ge volume fraction (%)	MSE
ASA 7	100	n/(1 0 0)	36.8 ± 0.2	19.5 ± 0.3	95 ± 1	30
ASA 8	100	p/(1 0 0)	34.0 ± 0.2	18.7 ± 0.3	96 ± 1	31.5
ASA 9	~80	n/(1 0 0)	42.0 ± 0.1	17.6 ± 0.6	72 ± 1	54
ASA 10	~80	p/(1 0 0)	39.4 ± 0.2	18.0 ± 0.5	53 ± 1	64.7
ASA 11	~60	n/(1 0 0)	35.7 ± 0.7	21.2 ± 0.4	21 ± 1	130
ASA 12	~60	p/(1 0 0)	37.8 ± 0.4	21.8 ± 0.3	34 ± 1	120
ASA 13	~40	n/(1 0 0)	32 ± 5	21 ± 5	8 ± 2	107.2
ASA 14	~40	p/(1 0 0)	26 ± 4	28 ± 3	6 ± 1	113

Table 2
Nominal Ge concentration, type and orientation of the substrates, layer thicknesses and composition obtained by spectroscopic ellipsometry and mean square error (MSE) of the fit using model "2"

Sample name	Nominal Ge concentration (%)	Type/orientation	Top SiO_2 thickness (nm)	(c-Ge + a-Ge + SiO_2) thickness (nm)	c-Ge volume fraction (%)	a-Ge volume fraction (%)	MSE
ASA 7	100	n/(1 0 0)	37.3 ± 0.1	17.9 ± 0.3	70 ± 2	33 ± 3	22.9
ASA 8	100	p/(1 0 0)	34.5 ± 0.2	17.2 ± 0.3	73 ± 2	31 ± 3	26.2
ASA 9	~80	n/(1 0 0)	43.3 ± 0.1	15.2 ± 0.3	56 ± 1	28 ± 2	32.1
ASA 10	~80	p/(1 0 0)	42.1 ± 0.2	19.7 ± 0.4	32 ± 1	36 ± 2	38.6
ASA 11	~60	n/(1 0 0)	44.7 ± 1.2	18.1 ± 0.1	0 ± 2	50 ± 5	120.8
ASA 12	~60	p/(1 0 0)	41.9 ± 1.3	21.8 ± 0.4	0 ± 2	49 ± 5	108
ASA 13	~40	n/(1 0 0)	31.3 ± 6	22.2 ± 5.5	7 ± 4	0 ± 3	107.3
ASA 14	~40	p/(1 0 0)	28.0 ± 5	26.3 ± 4.7	7 ± 4	0 ± 3	113.1

After breakdown the current drastically increased in forward direction, and *I–V* characteristics became Schottky-like, as presented in Fig. 2 for n-type sample ASA 11 with 60% nominal Ge content.

Nevertheless, p-type samples with nominal Ge contents of 40% (sample ASA 14) and 60% (sample ASA 12) exhibited a memory effect: a *C–V* hysteresis was obtained for both samples with a flat-band voltage shift of about 5 V for a bias range of 23 V, and about 7 V for a bias range of 18 V, respectively. The actual *C–V* characteristics are presented in Figs. 3 and 4, respectively.

A good homogeneity of the *C–V* hysteresis was obtained on sample ASA 14, as it can be seen in Fig. 3, where these results are presented for five different capacitors. However, it can also be seen that a part of the diodes exhibited instability at negative biases due to breakdown yielding high conductance in forward direction (sign of bias is referred to metal).

Capacitors on sample ASA 12 with 60% nominal Ge content endured high bias values for both directions, as can be seen in Fig. 4(a): they broke down at about 15 V forward biases. However, they showed some instability. The circle in Fig. 4(a) indicates the initial capacitance value of as-grown sample. Applying forward bias up to −15 V step-by-step, a virgin *C–V* curve was obtained (more abrupt solid curve). Due to hole injection at high forward voltages, the *C–V* curve was shifted to higher negative bias values, which was obtained decreasing the bias to zero step-by-step. When positive biases were applied up to +5 V (solid curve), a part of injected holes was escaped and

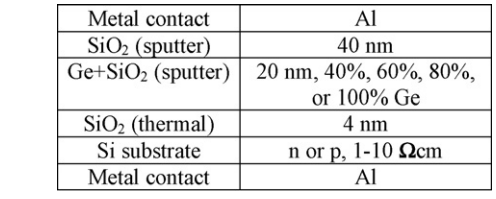

Fig. 1. Schematic of the studied Ge nanocrystal structures with different Ge content.

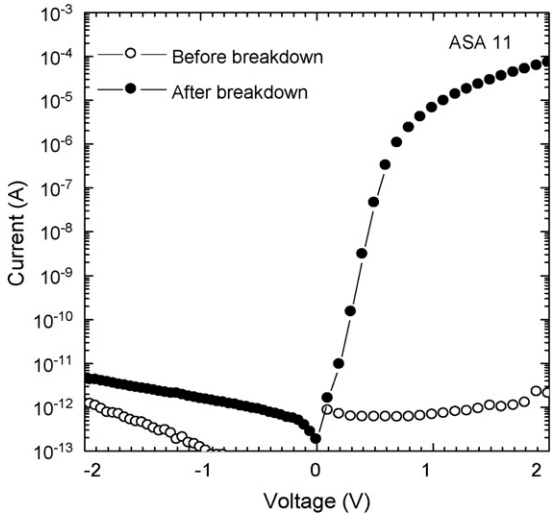

Fig. 2. Current–voltage characteristics obtained on the same capacitor on n-type sample ASA 11 with 60% nominal Ge content before and after breakdown.

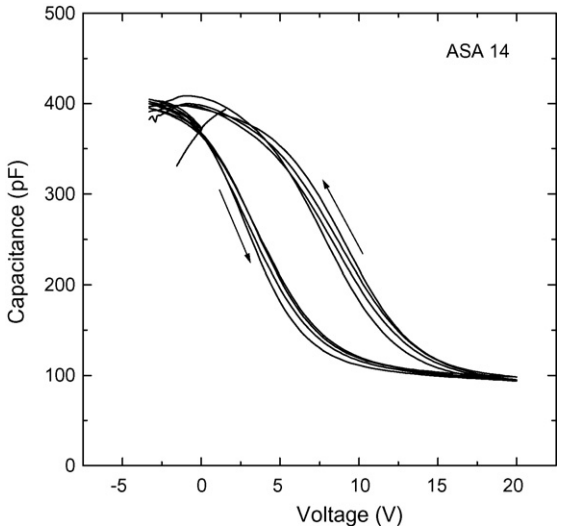

Fig. 3. Capacitance–voltage characteristics obtained on five different capacitors on p-type sample ASA 14 with 40% Ge content.

electrons were injected. However, when going back step-by-step to −15 V, a less abrupt *C–V* curve was obtained. This must be connected with escape of electrons injected at positive biases. In the next run, when the bias was increased to +15 V, a large shift was obtained due to electron injection (dashed line). But the *C–V* curve became even less abrupt, and electrons escaped from the structure even at positive biases. This behaviour indicates that electrons can escape easily from the structure.

The corresponding *G–V* curves obtained on sample ASA 12 for the same biases are presented in Fig. 4(b). Here the initial value is indicated with circle as well. Peaks correspond to the abrupt change of capacitance, when the Fermi-level sweeps along interface states yielding their charging–recharging process. For forward direction (negative biases) the conductance is high due to increasing leakage current. There is also a noise in the current, when the bias is increased in forward direction step-by-step, which can be attributed either to leakage as well, or to electron escape or hole injection into or from the nanocrystal layer. For reverse direction increasing positive biases yielded low conduction. These parts of the curves correspond to depletion, when there is no observable leakage.

The above results suggest that leakage current is limited by charge injection from Si, the role of charge injection from the metal electrode is negligible.

The samples with different Ge composition have been studied by spectroscopic ellipsometry as well. They were measured at four different angles of incidence (65.76°, 70.16°, 75.37° and 80.46°) between wavelength values of 250 nm and 820 nm. The evaluation of the spectra was performed on basis of a simple three-layer optical model. The model consists of three layers and an underlying single crystalline silicon substrate. The top and bottom layers (latter is adjacent to the substrate) were supposed to be stoichiometric SiO_2 layers with known dielectric spectra [14]. The thickness of the bottom layer was fixed at a value obtained on a reference sample that contained only this layer on top of the Si substrate. The thickness of the top layer was a fitting parameter.

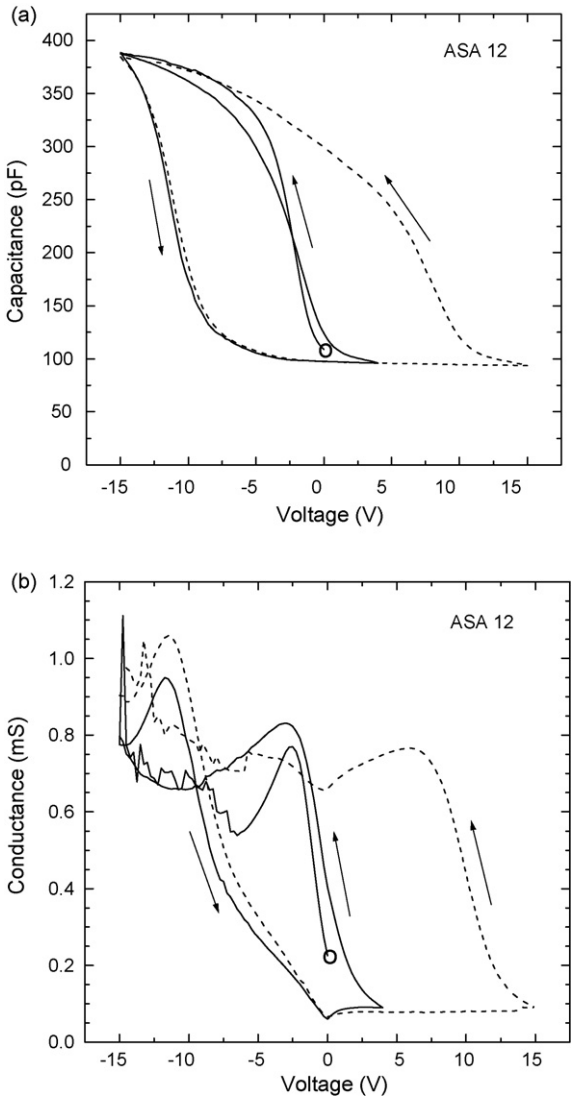

Fig. 4. Capacitance–voltage (a) and conductance–voltage (b) characteristics obtained on the same capacitor on p-type sample ASA 12 with 60% nominal Ge content for two different bias ranges. The initial capacitance and conductance values of as-grown sample are indicated by circle.

Two different models were used depending on the model for the middle layer. In the first model (model "1"), the middle layer was supposed to be a mixture of SiO_2 and crystalline Ge (c-Ge) [15]. The so-called effective medium approximation (EMA) ensures the background for this. In the second model (model "2"), this layer was supposed to be a mixture of SiO_2, crystalline Ge (c-Ge) [15] and amorphous (a-Ge) [16].

During the evaluation in case of model "1", three free parameters were considered: the thickness values of the SiO_2 as well as the mixed layer, and the volume fraction of c-Ge. The fit quality is characterized by the mean square error (MSE). The smaller the MSE the better is the fit quality. The results of the ellipsometric evaluation are shown in Tables 1 and 2.

The total thickness of the sputtered layers – as obtained by ellipsometry – is in the range of 52–64 nm. But for Ge contents of 40% and 60% the thickness of the Ge-containing layer is higher, than its nominal value of 20 nm. On the other hand, Ge

content is much less, than the nominal values in all samples. The less deviation from the nominal value was obtained for samples with 100% nominal Ge content. The origin may be either the non-stoichiometric composition of the SiO_2 layer, or the layer is not pure Ge. The fit quality for these samples is reasonable. In the case of 80% nominal Ge content the fit quality decreases, and the volume fraction of the c-Ge is significantly smaller than the nominal Ge content. For 40% and 60% nominal Ge contents the fit quality is poor, and the volume fraction of the c-Ge is much smaller than the nominal Ge content, in particular for 40% nominal value. The increased thickness of the Ge-containing layer and the thinner top layer suggest intermixing of these two layers during the sputtering or the annealing process.

Supposing that germanium is polycrystalline or nanocrystalline, a better approach can be found, if we consider this layer, as a mixture of three constituents: SiO_2, c-Ge and a-Ge (model ''2'', see Table 2). The background is that one can approach the dielectric function of certain polycrystalline materials, as the dielectric function of the mixture of single crystalline and amorphous materials. During the evaluation four free parameters were considered: the thickness values of the upper SiO_2 layer as well as the mixed layer, and the volume fraction of c-Ge, and that of a-Ge. The results extracted from data using this model, are given in Table 2. Except for the case of 40% nominal Ge content, the fit quality became better, than that for the previous model. This indicates that the middle layer contains amorphous Ge phase as well.

4. Conclusions

SiO_2 layer structures with a middle layer containing Ge nanocrystals have been prepared by sputtering on n- and p-type Si substrates with a thin oxide layer of 4 nm. Ge content in the middle layer has been varied in the range of 40–100%. The thickness and nanocrystal content of the layers were studied by spectroscopic ellipsometry, while their electrical behaviour by current–voltage, capacitance–voltage, and conductance–voltage measurements.

Most of the structures exhibited low breakdown voltages. The current through the structures became Schottky-like after breakdown. p-type samples with Ge content of 40% and 60% showed better breakdown properties and a considerable memory effect. It has been concluded that leakage current through the structures is limited by charge injection from Si, the role of charge injection from the metal electrode is negligible.

It has been obtained by spectroscopic ellipsometry that for 40% and 60% nominal Ge contents the volume fraction of the Ge is much smaller than the nominal Ge content. It has been concluded that the middle layer contains amorphous Ge phase as well. The results also suggest an intermixing of the layers during the sputtering or the annealing process.

Acknowledgements

This work has been supported by the European Commission in the frame of FP6 project SEMINANO with the contract no. NMP4 CT2004 505285, by the Hungarian Scientific Research Fund under grant no. T048696, and by Turkish Scientific Research Council (TUBITAK) with 104T520.

References

[1] C.L. Heng, N.W. Teo, V. Ho, M.S. Tay, Y. Lei, W.K. Choi, W.K. Chim, Microelectron. Eng. 66 (2003) 218–223.
[2] W.K. Choi, W.K. Chim, V. Ng, in: Semiconductor Nanocrystals, Proc. First Int. Workshop on Semiconductor Nanocrystals SEMINANO2005, Budapest, Hungary, September 10–12, 2005, vol. 1, 2005, pp.171–176, http://www.mfa.kfki.hu/conferences/seminano2005/.
[3] C.L. Heng, W.W. Tjiu, T.G. Finstad, Appl. Phys. A 78 (2004) 1181.
[4] G. Kartopu, V.A. Karavanskii, U. Serincan, R. Turan, R.E. Hummel, Y. Ekinci, A. Gunnæs, T.G. Finstad, Phys. Stat. Sol. (a) 202 (2005) 1472.
[5] C.L. Heng, T.G. Finstad, P. Storås, Y.J. Li, A.E. Gunnæs, O. Nilsen, Appl. Phys. Lett. 85 (2004) 4475.
[6] C.L. Heng, T.G. Finstad, Y.J. Li, A.E. Gunnæs, A. Olsen, P. Storas, Microelectron. J. 36 (2005) 531.
[7] S. Duguay, J.J. Grob, A. Slaoui, Y. Le Gall, M. Amann-Liess, J. Appl. Phys. 97 (2005) 104330.
[8] A. G. Rolo, A. Chahboun, M. I. Vasilevskiy, M. Stepikhova, M. J. M. Gomes, Semiconductor Nanocrystals; Proc. First Int. Workshop on Semiconductor Nanocrystals SEMINANO2005, 2005, Budapest, Hungary, September 10–12, vol. 2, 2005, pp. 283–286; http://www.mfa.kfki.hu/conferences/seminano2005/.
[9] A. Kanjilal, J. Lundsgaard Hansen, P. Gaiduk, A. Nylandsted Larsen, N. Cherkashin, A. Claverie, P. Normand, E. Kapelanakis, D. Skarlatos, D. Tsoukalas, Appl. Phys. Lett. 82 (2003) 1212.
[10] A. Dana, I. Akca, O. Ergun, A. Aydinli, R. Turan, T.G. Finstad, arXiv:-cond-mat/0605168 (2006).
[11] Zs.J. Horváth, Curr. Appl. Phys. 6 (2006) 145.
[12] Zs.J. Horváth, M. Ádám, I. Szabó, M. Serényi, Vo Van Tuyen, Appl. Surf. Sci. 190 (2002) 441.
[13] P. Basa, Zs.J. Horváth, T. Jászi, A.E. Pap, L. Dobos, B. Pécz, L. Tóth, P. Szöllősi, Physica. E 38 (2007) 71.
[14] E.D. Palik (Ed.), Handbook of Optical Constants of Solids, Academic Press, San Diego, 1998, p. 759.
[15] WVASE32 software, J.A. Woollam Co. Inc., 645 M Street, Suite 102 Lincoln, NE, USA 68508.
[16] A.A. Al-Mahasneh, Opt. Commun. 220 (2003) 129.